Rare Metal Materials and Engineering
Volume 50, Issue 3, March 2021
Available online at www.rmme.ac.cn

Science Press

Cite this article as: Rare Metal Materials and Engineering, 2021, 50(3): 0795-0801.

ARTICLE

Microstructure Characteristics and Tensile Strength of Aluminum/Stainless Steel Joint Welded by Inertia Friction

Liu Yong[1,2], Zhao Haiyan[1], Peng Yun[2], Ma Xiaofei[3]

[1] School of Materials Science and Engineering, Tsinghua University, Beijing 100084, China; [2] China Iron & Steel Research Institute Group, Beijing 100081, China; [3] School of Materials Science and Engineering, Shandong University, Jinan 250061, China

Abstract: Inertia friction welding (IFW) method is a potentially ideal technique to weld dissimilar materials. Aluminum and stainless steel were welded by inertia friction, and the morphology, microstructure, interfacial composition and mechanical properties of Al/steel joints were investigated. Results show that a thin intermetallic compound (IMC) reaction layer is found at the welding interface in the joint, and the IMC consists of Al, Fe and high concentration of Si. The microstructure of joint contains weld nugget zone, fully dynamic recrystallized zone (FDRZ), thermal mechanically affected zone and heat affected zone. The grain size of FDRZ is below 0.1 μm, and the average width of FDRZ in the joint is about 5 μm. The part with maximum hardness (HV) lies in FDRZ, and the maximum value is 3958 MPa in the joint. The tensile strength of joint is influenced by the rotational speed. When the rotational speed is 1100 r/min, the joint reaches to the maximum tensile strength of 323 MPa, which is related to the thickness of IMC at the weld interface.

Key words: inertia friction welding; dissimilar joint; microstructure; tensile strength

Dissimilar joints as aluminum alloy/stainless steel can combine the advantages of both materials and are widely used in many industries. However, the welding of aluminum and steel is difficult due to the differences in the chemical, mechanical and thermal properties of base metals[1-3]. Many welding methods are applied, but the joint results are still subject to some restrictions. Low solubility of Fe in Al results in the formation of thick and brittle intermetallic, which causes the degradation of mechanical properties.

Friction welding is a kind of solid-state welding method with low heat input[4-6]. Oxide films can be eliminated by the rubbing effect, and fresh aluminum alloy can be welded with steel by the frictional heat to obtain the good contact[7-9]. Heat generation in friction welding mainly depends on the process parameters of rotational speed and time[10]. According to the energy supply, the friction welding contains two methods: continuous drive friction welding (CDFW) and inertia friction welding (IFW)[11]. In CDFW, one part is attached to a rotating spindle reaching a constant rotation speed. In IFW, the rotating part is connected to a flywheel, and the rotating flywheel supplies the welding energy[12]. Previous studies achieved the joining between various metals, such as superalloy[13-15], titanium alloy[16], Al-Mg[17], Cu-Steel[18], and Al-steel[19,20]. The intermetallic compound (IMC) layer is controlled to be as thin as possible by adjusting the process parameters, and its critical thickness is 1~2 μm for the strong bond strength[21].

Dong et al[22] found that the IMC layer of rotary friction welded 5052 aluminum alloy/304 stainless steel dissimilar joints consists of Fe_2Al_5 and Fe_4Al_{13}, and the entire joint fractures through the interface and cracks mainly along the IMCs/5052 interface. The friction interface sequentially experiences three kinds of friction behavior before the initial peak torque: abrasion, slide and stick[23]. During the friction welding of Al and steel, Al experiences a large de-

Received date: March 16, 2020
Corresponding author: Zhao Haiyan, Ph. D., Professor, School of Materials Science and Engineering, Tsinghua University, Beijing 100084, P. R. China, Tel: 0086-10-62784578, E-mail: hyzhao@tsinghua.edu.cn

formation and forms the softened region in the heat affected zone (HAZ), and the large microstructural evaluation occurs[24,25]. There are four microstructural change zones at the Al side: base metal, heat-and-deformation-affected zone, interfacial zone, and solid solution zone[6].

In order to obtain high strength and good ductility of the joint, Fukumoto et al[26] found that enough heat cannot be generated within a short friction time, but the longer friction time causes the excess formation of IMC layers. The pure metal interlayer was applied to design the bimetallic structure for improving the metallurgical compatibility[27].

Mechanical properties of friction-welded dissimilar Al-steel joints are influenced by process parameters and working conditions[21]. Acceptable tensile strength and ductility can be obtained through the optimum process parameters[28-31]. To obtain the joint efficiency of 100%, joints should be made with the friction time of 1.5 s and the forge pressure of 240 MPa[10]. Sebastian et al[32] found that the bond strength shows a linear decrease with the increase of IMC thickness, but the variation in bond strength does not display a clear correlation.

IFW is a potentially ideal technique to weld the dissimilar materials of Al and steel. Microstructural evaluation and the control of IMC are the key issues for industrial application. The aim of this study is to develop a better understanding of the characteristics of Al/steel joints welded by IFW technique. The morphology, interface composition, microstructure and microhardness distribution of Al/steel joints were investigated.

1 Experiment

Base metals were 6061-T6 aluminum alloy (Al 6061) and 304 stainless steel (SS 304) in rod shape with diameter of 15 mm. A modified HSMZ-4 inertia friction welding was used to join the aluminum alloy and stainless steel. Before welding, rod surfaces were polished by SiC paper and then cleaned by acetone. Stainless steel rod was fixed on the rotary jaw, and the aluminum alloy rod was fixed on the stationary jaw. After the spindle was accelerated to the predetermined rotational speed, the motor was cut off automatically. Then the stainless steel rod rotated at a high speed with the spindle and the aluminum alloy rod moved axially under the constant axial pressure. Moment of inertia was 0.16 kg·m^2. The axial friction pressure was 180 MPa, and the rotational speed was 1100 r/min.

Specimen for microstructural observation was cut along the direction perpendicular to the welding interface by the electrical discharge machine. The SS 304 side was etched by the solution (2.5 mL HNO_3 and 97.5 mL ethanol), and the Al 6061 side was etched by the Keller's reagent (1.0 mL HF, 1.5 mL HCl, 2.5 mL HNO_3 and 95 mL H_2O). Microstructural characterization and elements distributions was carried out by optical microscope (OM), scanning electron microscope (SEM) and energy dispersive spectrum (EDS), transmission electron microscope (TEM) and electron backscattered diffraction (EBSD). Micro Vickers hardness test was carried out. The indentation load was 200 g and the dwell time was 10 s. Tensile property was measured by a universal testing machine at room temperature.

2 Results and Discussion

2.1 Morphology and interface of the welded joint

Fig.1 shows the morphology of the IFWed joint. After welding, the Al metal is extruded and causes asymmetrical deformation. The weld flash forms only at the Al side due to the decrease of the tensile yield of Al 6061 with increasing the temperature during welding, and the shape of flash depends on the friction welding parameters.

Al and Fe barely have mutual solubility leading to the formation of intermetallic compounds of Fe_xAl_x. The heat distribution is non-uniform in all directions of the interface, resulting in the formation of a non-uniform IMC layer. A very thin reaction layer is found between the stainless steel and aluminum alloy in the IFWed joint (Fig.1b). The thickness of the IMC layer of Al/steel joints majorly depends on the rotational speed and friction time[33]. This IMC layer is required to be as thin as possible[26,32].

Metallurgical bonds form as a result of the atomic diffusion across the joint interface. The IMC layer of Al/steel joint forms when the enough energy is provided at the weld interface. IFW can release the stored kinetic energy in a short time, which provides an instantaneous frictional heat for the diffusion of Al and Fe at the interface[34]. Fig.2 shows the elemental mapping of the Al/steel joint. It can be seen that Al, Fe and Si elements are diffused at the weld interface and form the IMC layer. Microstructural and elemental analysis of the joint interface shows the formation of a relatively non-continuous IMC layer in the IFWed joint.

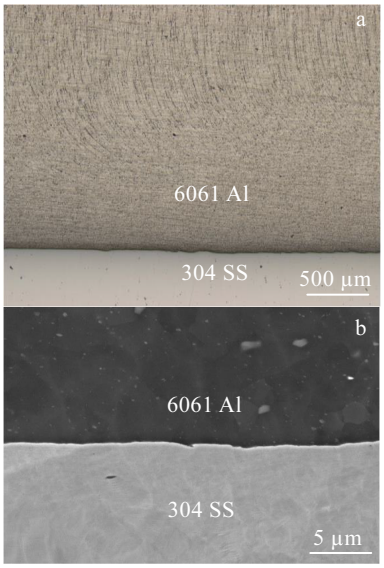

Fig.1 OM (a) and SEM (b) images of the welded Al/steel joint

The formation of the IMC layer at the weld interface is controlled by two major mechanisms of nucleation and growth[35]. Nucleation and growth of IMCs are both affected by the temperature and plastic deformation at the interface. In both methods, variation of the rotation speed influences the plastic deformation and the nucleation, which causes different thicknesses of IMC layer.

2.2 Microstructure of the welded joint

A clear weld interface is observed in the cross-section image, and the interface is relatively flat. Typical friction welded joint consists of four distinct zones: (1) weld nugget zone; (2) fully dynamic recrystallized zone (FDRZ); (3) thermal mechanically affected zone (TMAZ); (4) HAZ. Different temperatures and strains of these zones affect the final microstructures[11].

2.2.1 SS 304 side of Al/steel joint

Fig.2 shows the metallographic structure of the steel side in the Al/steel joint (Fig.2a). Few elongated grains are observed at the steel side (Fig.2b). During the friction welding, the interface temperature rises rapidly due to the thermal-mechanical coupling effect, which promotes aluminum alloy to experience recovery and dynamic recrystallization near the interface[22].

FDRZ is close to the interface. Fig.3 shows the EBSD image and grain size of the IFWed joint at the steel side. It can be seen that the microstructure in FDRZ changes into fine equiaxed grains compared to the base metal, and the formation of fine equiaxed grains, as a result of the frictional heat at the joint interface, is clearly observed. The grain size of FDRZ is below 0.1 μm (Fig.3b).

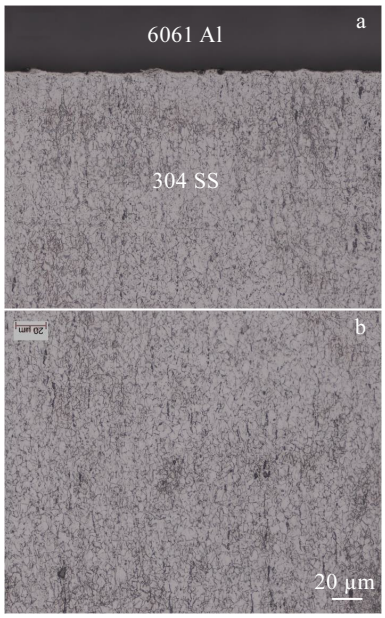

Fig.2 Microstructures of steel side in the Al/steel joint: (a) the Al/steel joint and (b) the steel side of joint

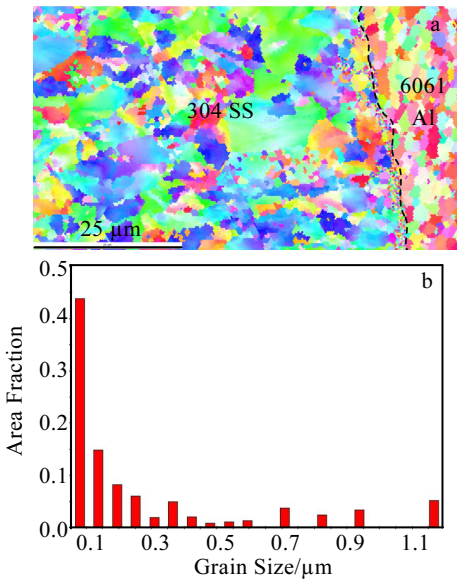

Fig.3 EBSD image (a) and grain size (b) of joint at the steel side

2.2.2 6061 Al side of Al/steel joint

Fig.4 shows the OM images of 6061 Al. In TMAZ, grains are elongated and bended. Matrix grains deform in TMAZ due to the plastic flow. The direction of plastic flow is clear. A large number of streamlines form, resulting in the rearrangement of strengthened particles. Because the amount of the second phase is high, the streamlines at the Al side are more obvious than those at the steel side.

Compared to the HAZ, the microstructure of the TMAZ suffers acute plastic deformation, inducing the appearance of deformed and elongated recrystallized grains. The grain size is 1~3 μm, and the width of FDRZ in the Al side is almost zero (Fig.5).

2.3 Microstructure and composition of IMC

Fig.6 shows the EDS element mapping of the Al/steel joint. It can be seen that Al, Fe and Si elements are diffused at the weld interface. IMC layer forms with a non-continuous morphology at the joint interface. Formation of the continuous or non-continuous IMC layer at the weld interface is controlled by two major mechanisms of nucleation and growth. Nucleation and growth of IMCs are both affected by the temperature and plastic deformation at the interface. The variation of rotation speed influences the plastic deformation and the nucleation during welding.

Fe and Al can form many kinds of IMCs. The Al-rich phases are mostly Fe_2Al_5 and $FeAl_3$, and the atomic ratios of Al to Fe are always larger than 3. In order to confirm the formation and composition of IMC, TEM observation was used to observe the detailed morphology and structure.

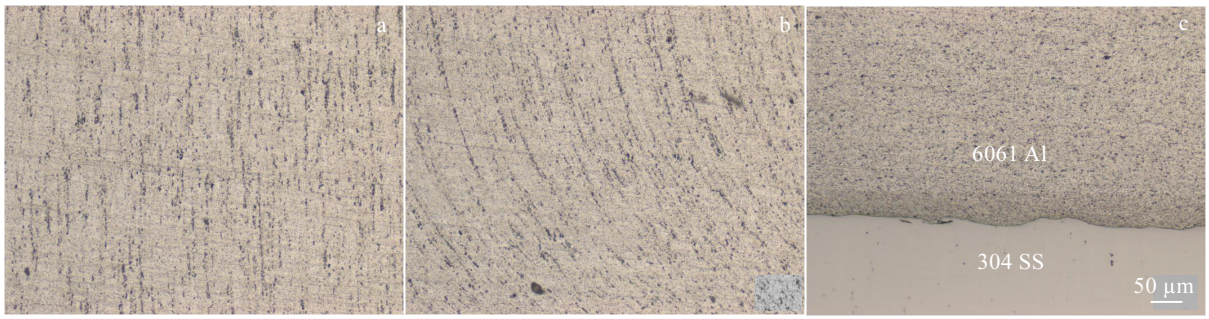

Fig.4 Microstructures of Al side in the Al/steel joint: (a) welding interface, (b) TMAZ, and (c) HAZ

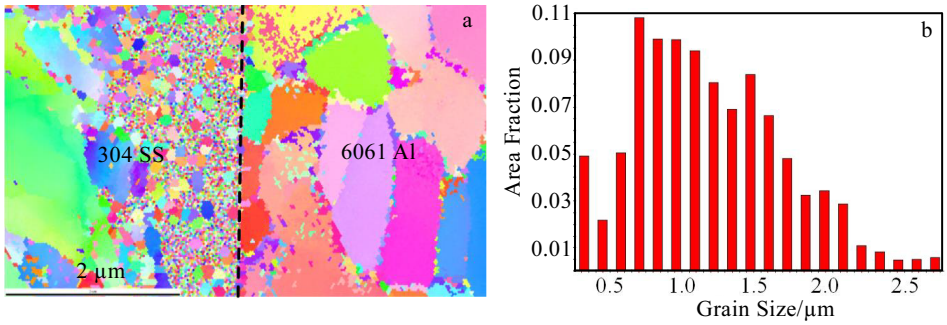

Fig.5 EBSD image (a) and gain size (b) of TMAZ and HAZ at the Al side

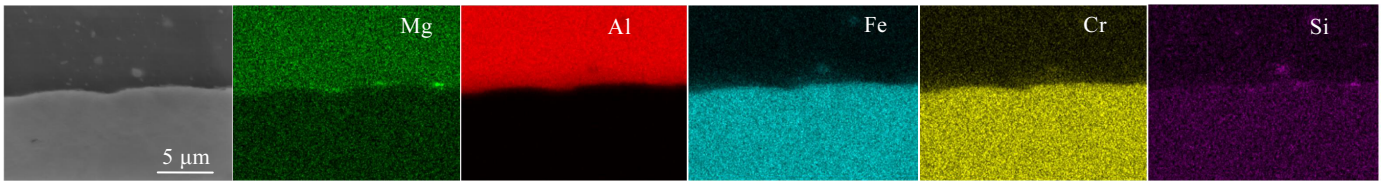

Fig.6 SEM image and EDS element mapping of the Al/steel joint

Fig.7a shows the bright field image of interface between 304 steel and 60601 Al alloy. During the friction welding, the interface temperature rises rapidly due to thermal-mechanical coupling effect, which promotes aluminum alloy to experience recovery and dynamic recrystallization near the interface. The metallurgical bonding is achieved in the welded Al/steel joint (Fig.7b). However, the continuous IMC is not found in the joint (Fig.7c).

Fig.8a shows the sparse IMC in the 6061 Al alloy side. The element composition results show that the atom ratio of Al to Fe is 3.07 (Point 5 of Table 1), which indicate that the IMC is $FeAl_3$. Fig.8b shows the selected area electron diffraction pattern of IMC, and the results confirm the formation of $FeAl_3$.

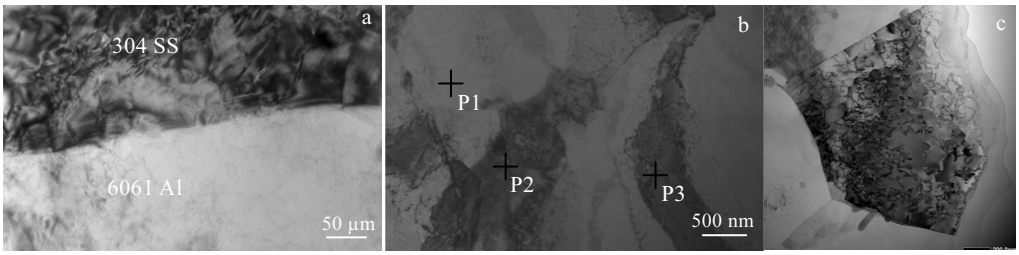

Fig.7 Interfacial microstructure of the Al/steel joint (a); microstructure close to the steel side (b); microstructure close to Al side (c)

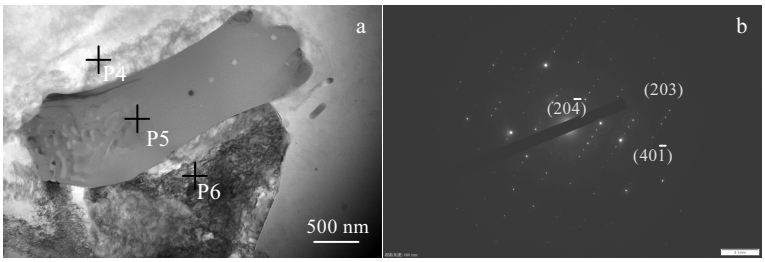

Fig.8 Sparse IMC in the 6061Al alloy side (a) and the SAED pattern of IMC (b)

Table 1 EDS analysis results of different points in Fig.7b and Fig.8a (at%)

Point	Al	Fe	Mg	Si	Cr	Mn	Ni
P1	1.14	69.79	-	1.25	17.99	1.15	8.69
P2	1.20	70.83	0.02	-	18.20	1.17	8.58
P3	0.93	69.43	-	1.38	18.31	1.21	8.75
P4	96.10	1.56	0.90	0.74	0.63	-	0.07
P5	67.91	22.10	0.10	6.14	1.44	1.80	0.52
P6	95.91	1.87	1.02	0.37	0.59	0.16	0.08

Fig.9 shows the element mapping results of the sparse IMC. The interfacial structure consists of an IMC with Si enrichment (Table 2). The local Si enrichment layer forms along the interface, and the high concentrated Si can promote the formation of non-uniform IMC layer[36]. According to Fig.8 and 9, and EDS analyses (Table 1 and Table 2), the IMC should be $FeAl_3$ with Si enrichment.

2.4 Hardness of the welded joint

Fig.10 shows the microhardness distribution of the joint. Because physical and chemical properties of base metals are different, the hardness of SS 304 is about 3 times higher than that of the Al 6061 base metal. The hardness reaches to the maximum value in the FDRZ at the steel side. The maximum hardness (HV) is 3958 MPa in the IFWed joint. The microhardness of joints may be affected by the combination of the following factors: modification of microstructure, dissolution of strengthening phases, and grain size. The main reason should be related to the eutectics and recrystallized fine grains as an effect of heat input and rotational speed during different friction welding processes. In addition, the microhardness is hard to measure in the narrow FDRZ in the IFWed joint, which is also a reason for the relatively low maximum hardness in the IFWed joint. In the Al base metal, the average hardness is 1015 MPa, while the average hardness in HAZ is 760 MPa. This reduction in hardness is due to the eutectics and recrystallized fine grains as an effect of heat input and rotational speed during friction welding.

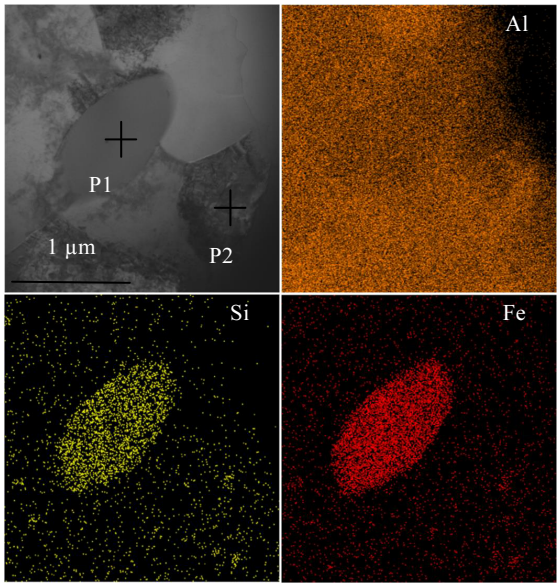

Fig.9 EDS element mapping of the sparse IMC in the Al/steel joint

Table 2 EDS analysis results of different points in Fig.9a (at%)

Point	Al	Fe	Mg	Si	Cr	Mn	Ni
P1	64.57	24.22	0.07	5.97	2.19	2.21	0.77
P2	96.18	1.40	1.21	0.52	0.53	0.08	0.08

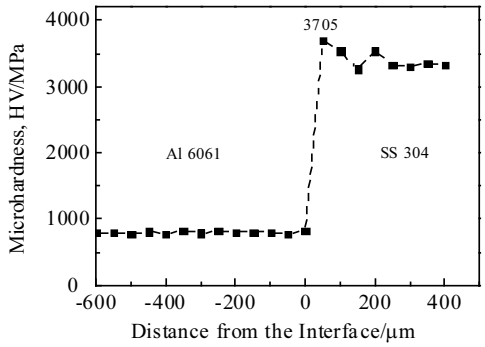

Fig.10 Hardness profile of the welded joint

2.5 Tensile strength of the welded joint

In the IFWed joint, the tensile strength gradually increases due to the increase of rotational speed, and reaches to the maximum tensile strength of 323 MPa, which is about 92% of the tensile strength of Al 6061 base metal (Fig.11). When the rotational speed continues to increase, the joint strength starts to decrease. The high tensile strength is due to the thickness of IMC at the weld interface. The thick, continuous and hard IMC layer provides the potential initiation of crack. The thick layer of IMCs deteriorates the tensile strength and ductility of the joint. The analysis of the Al-steel interface is critical due to the formation of brittle IMCs at this location.

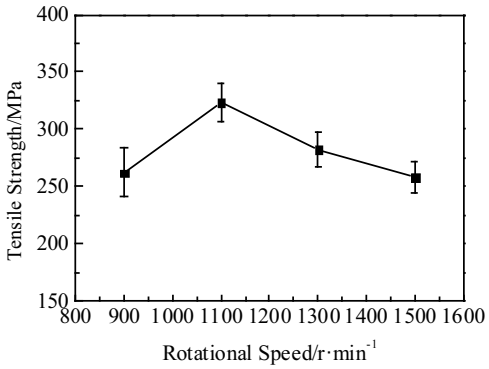

Fig.11 Relationship between tensile strength and rotational speed for the joint

3 Conclusions

1) Al 6061 and SS 304 exhibit good axial symmetry and consistent flying edge at the interface in the joint. A thin reaction layer is found between stainless steel and aluminum alloy in the joint.

2) In the SS 304 side of Al/steel joint, few elongated grains are observed and the fully dynamic recrystallized zone (FDRZ) is close to the interface. The average width of FDRZ at steel side in the joint is about 5 μm. The grain size of FDRZ is below 0.1 μm. At the Al 6061 side of Al/steel joint, grains are elongated and bended, and the streamlines at the Al side are more obvious than those at the steel side in thermal mechanically affected zone (TMAZ). The non-uniform IMC layer forms at the joint interface. The IMC should be $FeAl_3$ with Si enrichment. The high concentrated Si can promote the formation of IMC layer.

3) The hardness (HV) reaches to the maximum value in the FDRZ at the steel side, which is 3958 MPa. The maximum tensile strength of joint is 323 MPa, which is about 92% of the tensile strength of Al 6061 base metal. The reason is related to the thin IMC at the weld interface.

References

1 Shah L H, Ishak M. *Materials and Manufacturing Processes*[J], 2014, 29(8): 928
2 Derazkola H A, Khodabakhshi F. *The International Journal of Advanced Manufacturing Technology*[J], 2019, 100(9): 2401
3 Wang P X, Chen Q P, Pan Q H *et al*. *The International Journal of Advanced Manufacturing Technology*[J], 2016, 87(9): 3081
4 Huang Y, Wan L, Si X *et al*. *Metallurgical and Materials Transactions A*[J], 2019, 50(1): 295
5 Sun G Q, Xu G S, Shang D G *et al*. *Welding in the World*[J], 2019, 64: 1
6 Wan L, Huang Y. *The International Journal of Advanced Manufacturing Technology*[J], 2018, 95(9): 4117
7 Meshram S D, Mohandas T, Reddy G M. *Journal of Materials Processing Technology*[J], 2007, 184(1): 330
8 Huang Y, Huang T, Wan L *et al*. *Journal of Materials Processing Technology*[J], 2019, 263: 129
9 Yılmaz M, Çöl M, Acet M. *Materials Characterization*[J], 2003, 49(5): 421
10 Kimura M, Suzuki K, Kusaka M *et al*. *Journal of Manufacturing Processes*[J], 2017, 26: 178
11 Li W, Vairis A, Preuss M *et al*. *International Materials Reviews*[J], 2016, 61(2): 71
12 Ding Y, You G, Wen H *et al*. *Journal of Alloys and Compounds*[J], 2019, 803: 176
13 Preuss M, Withers P J, Baxter G J. *Materials Science and Engineering A*[J], 2006, 437(1): 38
14 Zhang C, Shen W, Zhang L *et al*. *Journal of Materials Engineering and Performance*[J], 2017, 26(4): 1581
15 Wang F F, Li W Y, Li J L *et al*. *The International Journal of Advanced Manufacturing Technology*[J], 2014, 71(9): 1909
16 Turner R P, Perumal B, Lu Y *et al*. *Metallurgical and Materials Transactions B*[J], 2019, 50(2): 1000
17 Guo W, You G, Yuan G *et al*. *Journal of Alloys and Compounds*[J], 2017, 695: 3267
18 Luo J, Liu S, Chen W *et al*. *Materials and Manufacturing Processes*[J], 2016, 31(3): 275
19 Fauzi A M N, Uday M B, Zuhailawati H *et al*. *Materials & Design*[J], 2010, 31(2): 670
20 Hynes N R J, Velu P S. *The International Journal of Advanced Manufacturing Technology*[J], 2017, 93(1): 121
21 Mehta K P. *Journal of Materials Research*[J], 2019, 34(1)
22 Dong H, Li Y, Li P *et al*. *Journal of Materials Processing Technology*[J], 2019, 272: 17
23 Li P, Li J, Li X *et al*. *Journal of Adhesion Science and Technology*[J], 2015, 29(12): 1246
24 Maalekian M. *Science and Technology of Welding and Joining*[J], 2007,12(8):738
25 Luo J, Ye Y H, Xu J J *et al*. *Materials & Design*[J], 2009, 30(2): 353
26 Fukumoto S, Tsubakino H, Okita K *et al*. *Materials Science and Technology*[J], 1999, 15(9): 1080
27 Cheepu M, Che W S. *Transactions of the Indian Institute of*

Metals[J], 2019, 72(6): 1597
28 Kimura M, Ishii H, Kusaka M *et al*. *Science and Technology of Welding and Joining*[J], 2009, 14(7): 655
29 James J A, Sudhish R. *Procedia Technology*[J], 2016, 25: 1191
30 Kimura M, Kusaka M, Kaizu K *et al*. *The International Journal of Advanced Manufacturing Technology*[J], 2016, 82(1): 489
31 Wang T, Sidhar H, Mishra R S *et al*. *Science and Technology of Welding and Joining*[J], 2019, 24(2): 178
32 Herbst S, Aengeneyndt H, Maier H J *et al*. *Materials Science and Engineering A*[J], 2017, 696: 33
33 Fukumoto S, Tsubakino H, Okita K *et al*. *Scripta Materialia*[J], 2000, 42(8): 1
34 Rathod M, Kutsuna M. *Welding Journal*[J], 2004, 83(1): 16
35 Fereiduni E, Movahedi M, Kokabi A H. *Journal of Materials Processing Technology*[J], 2015, 224: 1
36 Shen Z, Chen J, Ding Y *et al*. *Science and Technology of Welding and Joining*[J], 2018, 23(6): 462

铝合金/不锈钢惯性摩擦焊接头的组织特性和力学性能研究

刘　永[1,2]，赵海燕[1]，彭　云[2]，马肖飞[3]
(1. 清华大学 材料学院，北京 100084)
(2. 钢铁研究总院 先进钢铁流程及材料国家重点实验室，北京 100081)
(3. 山东大学 材料科学与工程学院，山东 济南 250061)

摘　要：惯性摩擦焊是一种连接异种金属理想的焊接方法，对铝合金/不锈钢采用惯性摩擦焊进行焊接，并详细研究了焊接接头的形貌、组织、界面成分和力学性能。结果表明，在惯性摩擦焊接头的界面处形成了很薄的金属间化合物（IMC）反应层，该反应层主要由 Al、Fe 元素组成，是富集 Si 元素的 $FeAl_3$ 相。惯性摩擦焊接头组织由焊核区、完全动态再结晶区、热机械影响区和热影响区组成。完全动态再结晶区的晶粒尺寸小于 0.1 μm，它的平均宽度为 5 μm。接头的显微硬度（HV）最大值出现在不锈钢侧的完全动态再结晶区，其值为 3958 MPa。惯性摩擦焊中，初始转速对接头的拉伸性能有显著影响。当初始转速为 1200 r/min 时，铝/钢惯性摩擦焊接头的最大抗拉强度为 323 MPa，达到铝合金母材强度的 92%。

关键词：惯性摩擦焊；异质接头；微观组织；抗拉强度

作者简介：刘　永，男，1974 年生，博士生，清华大学材料学院，北京　100084，电话：010-62784578，E-mail: liuyong1350130711@126.com